A NEW APPROACH FOR THE DETERMINATION OF ONSET OF FAILURE POINTS DURING LABORATORY STRENGTH TESTING OF ROCKS

Deniz MAMUREKLI

Zubeyde Hanim Cad. No=92/3 Karsiyaka, 35530 İzmir, Turkey
Corresponding author's e-mail: sdeniz.mamurekli@bayar.edu.tr

ABSTRACT
Estimating the pre- failure points for rocks during laboratory testing is not a trivial task. In this study, a new approach is introduced that utilizes change in the slope of the load-deformation curves of rock in the loading cycle for marking the onset of failure point during uniaxial test of a given rock. At each step, load-deformation data footprints of the rock under test are inspected and a decision is made whether the failure has started or not. The load-deformation data obtained from different tests of different rocks are examined including; Norite, Granite, Limestone, Sandstone, Siltstone and Marble. The computational results over 154 cored rock samples show that the proposed approach locates the onset of failure point for a given rock with an acceptable degree of accuracy.

KEYWORDS: pre-failure points, uniaxial tests, load-deformation

INTRODUCTION

The accurate determination of strength and stiffness properties of rock is vital in many Rock Mechanics investigations. The strength of a cored-rock can be determined in a laboratory using a variety of methods, such as uniaxial and triaxial compressive strength tests. Rocks show a wide range of stress-strain behaviour as they approach to failure. Over the past forty years, the deformation and fracture characteristics of tested rock have been studied by many researchers including (Mogi, 1966; Bieniawski, 1967; Perkins et al., 1970; Wawersik and Fairhurst, 1970; Lajtai, 1972; Lama and Vutukuri, 1972; Tapponnier and Brace, 1976; Ramamurthi, 1986; Ofoegbu and Curran, 1992; Martin and Chandler, 1994; and Eberhardt, et al., 1999).

The standard single-stage triaxial test requires a large number of specimens to obtain the complete strength envelope in which a confining pressure is set and the axial load is applied until a small cored-rock sample fails. In multi-stage triaxial test (MSTT), potential failure point of a tested sample is identified ahead of its failure (pre-failure point), and then the confining pressure is increased to the next level before the total failure occurs. This process requires a high level of experience to be carried out successfully, particularly for relatively brittle rock material. There have been some previous studies on the pre-failure behaviour of rocks under compression as exemplified in the literature (Yoshinaka et al., 1983; Yumlu and Ozbay, 1995; Katz and Reches, 2002; Lei, 2006; Dweirj, 2006). Dweirj (2006) developed a real time approach for the detection of the failure point of a rock specimen in a UCS test or the first stage of MSTT at zero confinement (σ_3=0) before a complete rupture of a sample occurred. This method is based on the identification of change in the gradient of the load-deformation (L-D) curve aided by a curve smoothing technique for reducing the distortion along the curve. This method is currently employed on the stiff press rock testing machine at the Nottingham Centre of Geomechanics, University of Nottingham.

In this study, the load-deformation data of over 154 cored-samples of several rock types are used for estimating onset of failure points during uniaxial compressive strength (UCS) tests. The historical L-D data is put onto test by a computer program developed in C programming language and based on calculation of the slope of the L-D during loading cycle of the test using raw data. The proposed approach confirmed well with any type of L-D curve subject to the condition that it follows a familiar geometry representing the overall test of failure. The onsets of failure points detected by the program are less than 5 % of slip which makes the program ideal for the determination of close points to maximum resistance.

IDENTIFYING CHARACTERISTICS OF LOAD-DISPLACEMENT CURVES

Identifying characteristics of L-D curves plays an important role in predicting the uniaxial compressive strength of a material. Figure 1 shows some of the L-D curves for different type of rocks tested. As it can be observed, not only different type
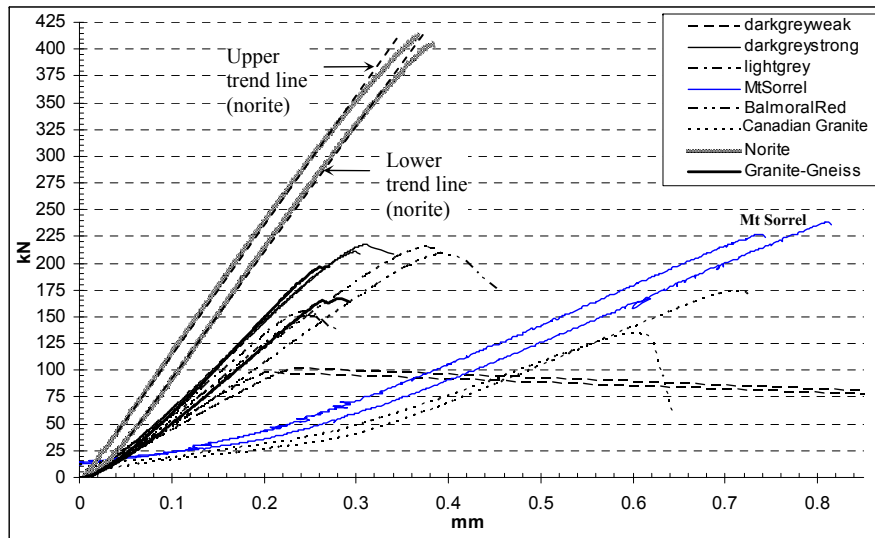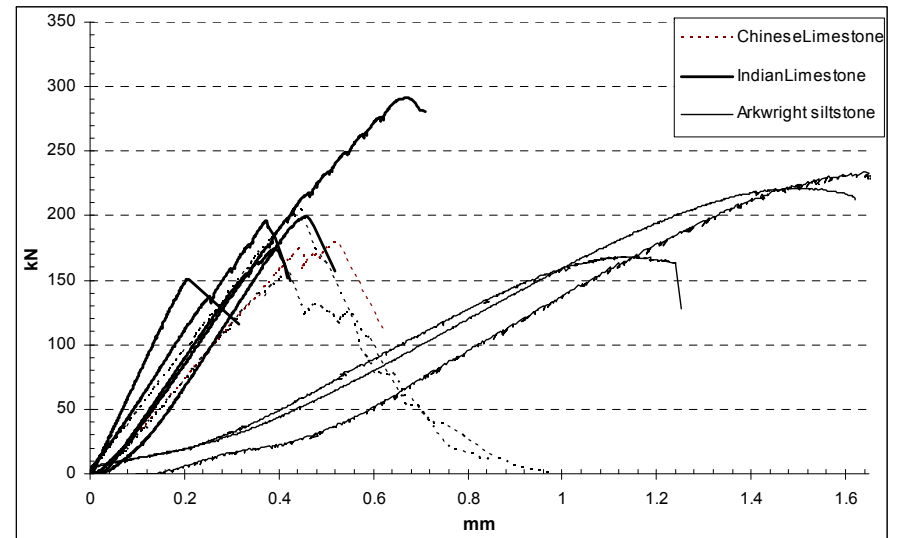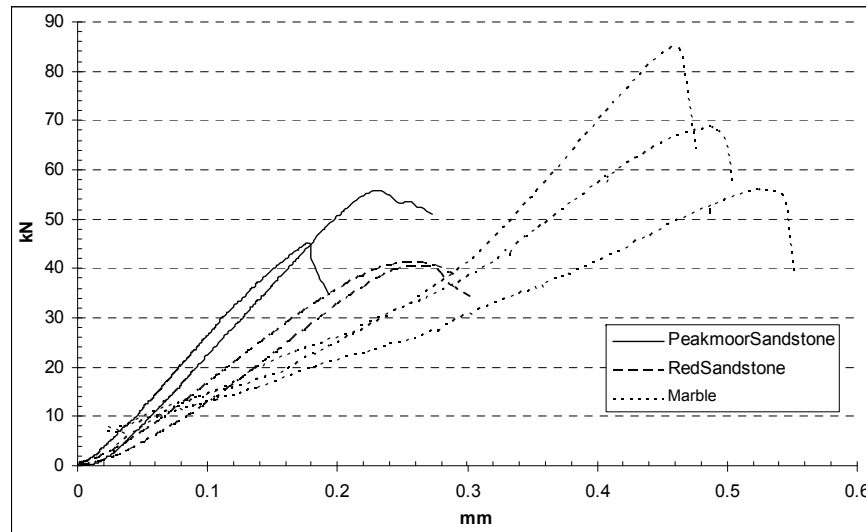
Fig. 1   Load-deformation curves of different rock samples tested (after Reddish, 2008).
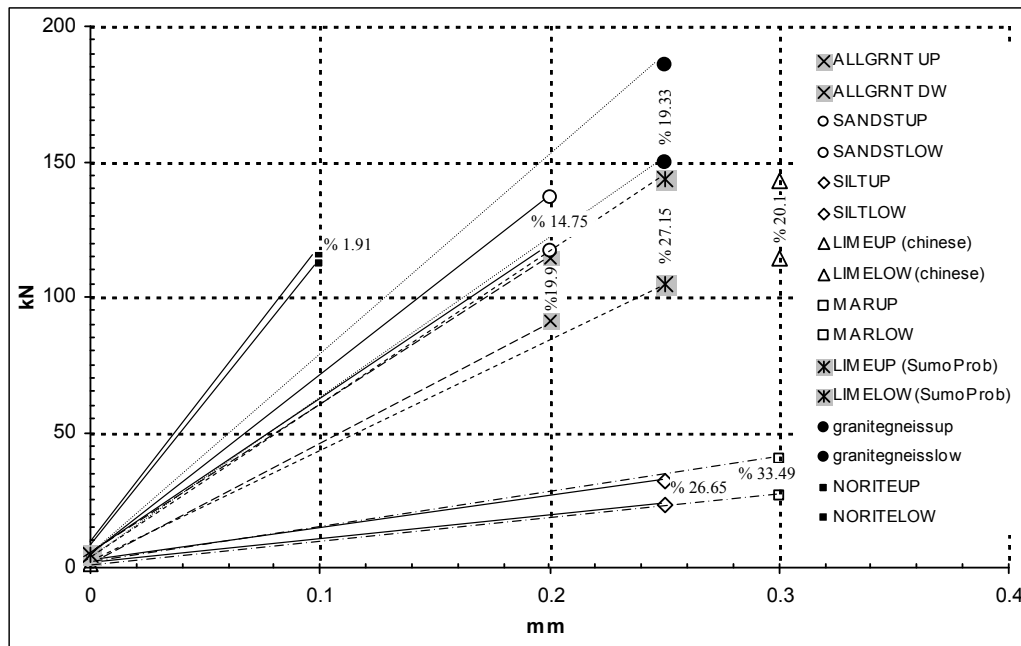
Fig. 2 Upper and lower trend lines and percents of deflection of different kinds of rock samples tested.

of rocks but also, different samples of the same type of rock show dissimilar characteristics. Although each curve exhibits a similar behaviour within the same group of rock, in most of the cases, variation of onset of failure points is significant. Therefore, it is necessary to identify the behaviour of L-D data of the curves to reflect the differences between similar curves.

The stress-strain behaviour of a loaded material can be linked to the stages of opening and closing of cracks in a material. These stages can be defined as: crack closure, linear elastic deformation, crack initiation and stable crack growth, critical energy release and unstable crack growth and failure and post peak behaviour (Dweirj, 2006). This study mainly focuses on the linear elastic deformation and immediately there after where crack initiation and stable crack growth stage starts. In the first part of the study, L-D characteristics of norite, granite, sandstone, limestone, marble and siltstone dry rock samples were studied to understand the behaviour of L-D curves. Cylindrical samples were cored in vertical orientation from the same block of rocks. The samples were prepared for the UCS tests to comply with the International Society of Rock Mechanics (ISRM) suggested standards. In Figure 1, L-D curves of different rock samples show variations in rising trends and failure locations.

Figure.1a illustrates the rising trend of L-D curves, which defines the linear behaviour of the rock, this declines as the rock's physical properties change from very hard (norite) to hard (granite-gneiss, dark-grey granite) and medium hard rocks such as MtSorrel

and BHP granites. It is observed that the variation on the trend line does not provide any evidence for determining onset of failure points. Apart from Mt.Sorrel granite samples, L-D data paths of other group of rocks are in regular trend due to a less discordant and stiff-bonded structure of the rock types. In Figure 1b, L-D data paths of the rocks are in irregular trend and show different points of failure. Siltstone samples especially show undulated data paths confirming a jagged type of L-D pattern. The graphs of sandstone and marble samples show considerable variations in L-D data path with lower trend lines and changing points of failure (Fig. 1c). In the second part of the study, the trend lines of L-D data of all samples were studied. The deflection percentages between points located on the uppermost and lowermost trend lines of L-D curves are depicted in Figure 2. The deflection percentages show wide variations according to rock types tested. The percentages of deflection increase with lower rock stiffness and weaker bonding texture. The upper and lower trend lines explain the rock stiffness scale so that the harder the rock types the steeper the upper and lower lines become.

STUDIES FOR DETERMINATION OF ONSET OF FAILURE POINTS

The boundary zone between elastic and plastic behaviour of the rock samples under loading should be carefully detected for establishing onset of failure points. Yielding, eventually, leads to the irreversible deformation of a given rock at some point within the plastic zone during a compression test. Hence,
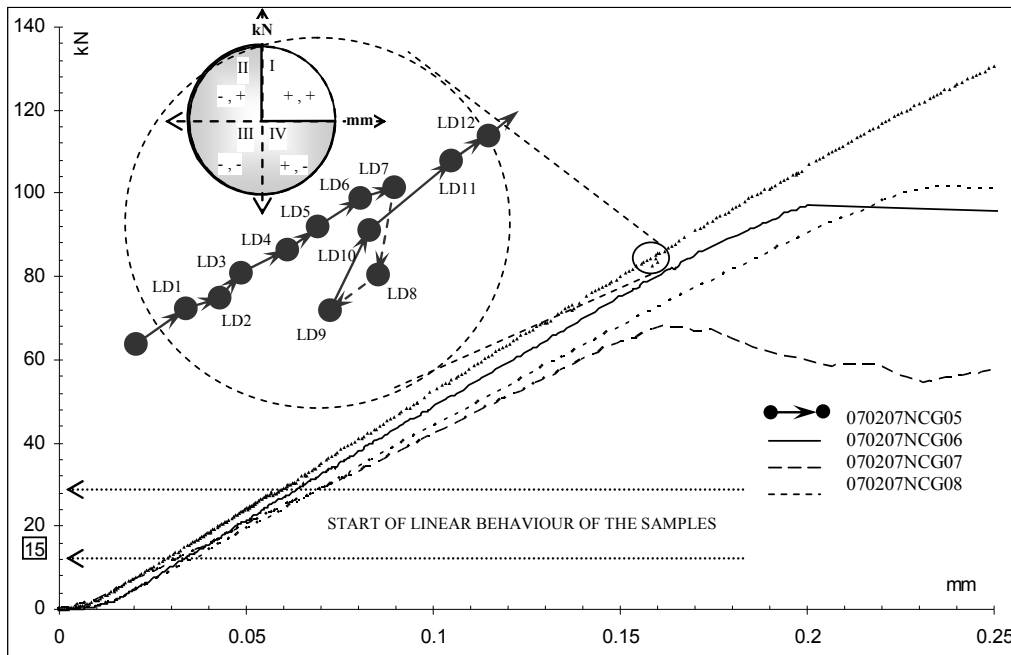
Fig. 3 Picking of rising trend lines of L–D data of a weak dark-grey granite sample.

a warning is beneficial for the person who is conducting test in order to stop loading further before such a failure occurs. This is the position at which the optimum onset of failure point is reached.

From the understanding of L-D data behaviour, curve fitting was practiced on all tested dry rock samples during the studies. A third degree function was searched using the test data hoping that it would be the best descriptor of L-D behaviour for the rock samples. However, no third degree descriptive function can be found that would represent all L-D data paths, even for the same type of rock samples. Therefore, the study was concentrated on identifying the L-D data behaviour at different segments of the graph path. All rock samples under uniaxial loading have a common functional shape; a settlement part which curves in, an elastic section which is in linear rising trend and a plastic part where progressive yielding leads to failure, respectively. Since the onset of failure points is expected to be located where linear behaviour of the rock ends, the research was focused on distinctions of L-D data functioning at elastic-plastic boundary of the graph. The limits of this boundary vary depending on the rock type tested providing less data before failure so making difficult to locate onset of failure points especially for highly brittle rocks in contrast to ductile rocks.

The slope picking process starts just after linear behaviour of the rock begins. The averaged rising trend line alters significantly in early development of slope accumulation showing a little effect on its orientation as the load builds up in later stages of the L-D test. The slopes of L-D data have a tendency to decrease as deformation of the rock changes from elastic to permanent. After this point, onset of failure point can be determined when a few successive L-D data slopes (inside the first quadrant of trigonometric circle) decline from the orientation of the averaged rising trend line declining below a threshold (≥ 15 per cent). A slope picking process and development of the rising trend line representative of L-D data of a dark-grey granite (weak) sample is depicted in Figure 3.

COMPUTER PROGRAM FOR DETERMINING ONSET OF FAILURE POINTS

Figure 4 illustrates the fluctuations of the connected neighbouring slopes. The slopes located inside the first quadrant of trigonometric circle (slopes positive and rising) are taken into account. Those slopes are averaged to constitute the average slope line which alters with every contribution of new input; L-D test datum. As the incoming data accumulates progressively the representative trend line shows slight changes with rise and fall of data slopes till it closes up to the end of elastic deformation zone. Sometimes, these L–D data changes may appear as small ring-shaped undulations or wavy on the path of rising trend line changing with the rock type tested under unchanged loading type and regime conditions. Considering these occasional L–D data changes are not the indication of nearing to the onset of failure locations, the slope fluctuations occurring apart from inside the first quadrant of trigonometric circle are discarded. The slopes located inside the first quadrant of trigonometric circle are averaged to form the averaged trend line. Subsequently, the trend line
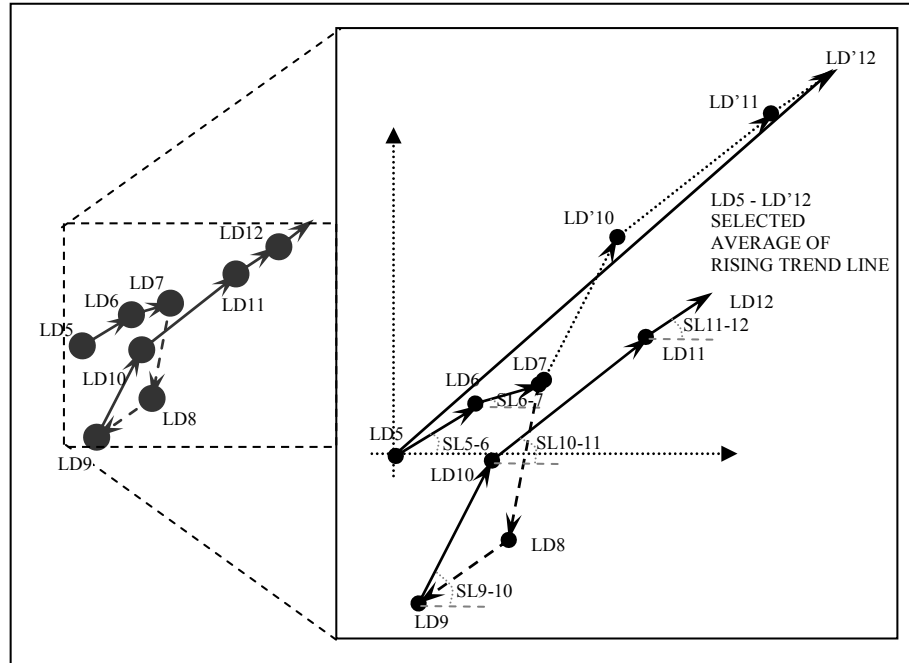
Fig. 4   Selected average of rising trend line (LD5–LD'12) of L–D data of a dark-grey granite sample.

declines in slope along with continuous slope drops of incoming data when the load approaches to the onset of failure point. In Figure 4, a part of real-time L-D data of a dark-grey granite sample's trend line is shown, introducing the fundamental logic behind the developed approach. During the application of the developed approach, the slopes of SL_{5-6}, SL_{6-7}, SL_{9-10}, SL_{10-11} and SL_{11-12} (solid arrow lines) are accepted while SL_{7-8} and SL_{8-9} slopes (dashed arrow lines) located inside the third quadrant of trigonometric circle are discarded.

In estimation of the onset of failure points, a software program was required to make the approach work quickly on L-D test data. In this stage, the pre-recorded load and displacement data is inputted from a text file together with a determined initial load [where elastic deformation of rock sample is believed to be started]. The program ignores all L-D data prior to a given starting load of elastic deformation. Furthermore, a distinctive trend line, composed of average of rising L-D figures, is steadily formed by the accumulation of incoming data. This line helps to detect successive slope-drop differences of neighbouring data in plastic deformation zone where onset of failure point is anticipated to be determined by the program. The pseudocode of the algorithm is provided in Figure 5.

The trend line constitution procedure and correlation of slope-drop differences of incoming data with the trend line continues until the program approximates to onset of failure point or reaches the end of file. If the end of file is reached without identifying a pre-failure point, a warning message is issued as "no onset of failure point detected". During the experiments, existing files with full content were utilized, but the proposed algorithm is fast enough (≤1s) to process real-time data.

EXPERIMENTAL DATA AND RESULTS

Data used for this research was supplied from the Nottingham Centre for Geomechanics Rock Test Database (Rowsell, 2005 and Reddish, 2008). The database comprises a large number and variety of rock test results (UCS, Tri-axial single stage and Tri-axial multi stage) as well as other rock properties. The compression tests conducted by the Nottingham Centre for Geomechanics used the following set up.

1) Testing System

The tests were carried out on the cored rock samples using servo-controlled stiff press testing machine originally manufactured by RDP-Howden which has a capacity of 1000kN and can be used to determine mechanical properties of rocks, resins, and support elements such as rock bolts. The stiff press testing machine is made up of a four column straining frame with adjustable cross-head position, incorporating a double acting servo-control-led actuator. The actuator is designed to apply a maximum tensile and compressive load of 1000kN over a total working stroke of 100mm. PC computing logger records all the transducer feedback signals. The recorded readings can be stored on external storage devices (HD, FD etc.) for further data analysis (Rowsell, 2005).

Algorithm: Onset of Failure of L-D Points Identification

Input: File_name (txt), Linear_Behaviour_Start (constant)
Output: Onset_of_failure_load, Onset_of_failure_displacement
Begin
1.   Initialize previous main load and main displacement values: $Ram\_Load_{previous} = 0$, $Displacement_{previous} = 0$;
2.   **repeat** // process data line by line from the file or (from the test machine)
3.   Read a line from the file: $Ram\_Load_{current}$ and $Displacement_{current}$;
4.   **if** ($Ram\_Load_{current} > 0$ **and** $Ram\_Load_{current} > Ram\_Load_{previous}$) **then**
5.   **if** ($Ram\_Load_{current} <$ Linear_Behaviour_Start) **then**
6.   Set the new slope to 0;
7.   **else**
8.   Compute the new slope;
9.   Add the new slope to the previously accumulated slope values ;
10.   Calculate overall average slope, $avr\_slope_{current}$;
11.   Use the previous value of the accumulated slope, $sum\_slope_{previous}$
12.   **if** (($sum\_slope_{previous} > 0$) **and** *percentageDeviation*($sum\_slope_{previous}$, $avr\_slope_{current}$)>0) **and**
13.   *percentageDeviation*(new slope, $avr\_slope_{previous}$) > threshold)) **then**
14.   Onset_of_failure_load = $Ram\_Load_{current}$;
15.   Onset_of_failure_displacement = $Displacement_{current}$;
16.   **break;** // out of the repeat-until loop since a pre-failure point is detected
17.   **else**
18.   Set the previous values to current ones;
19. **until** (end_of_file)
20. **if** (Onset_of_failure_load **and** Onset_of_failure_displacement are set) **then**
21.   Print (Onset_of_failure_load, Onset_of_failure_displacement)
22. **else**
23.   Print ("no onset of failure point detected")
End

Fig. 5   Pseudocode of the onset of failure identification algorithm.

2) Testing System Control

The testing machine was controlled with a Windows-based system, coded in MS Visual Basic. The control software package allowed the user to customise any test requirement by providing an easy and common user interface. Both the ramping and the confining pressure rates and values could be assigned for each test step separately allowing flexibility to conduct more complex testing procedures. The load rate for the samples was less than 1.5 kN/s, and the average load rate was around 0.5 kN/s. 3 to 10 points were recorded for each 1kN of load applied (Rowsell, 2005). The applied load changes against piston displacements of some samples of various rock types tested are presented in Figure 6. As it can be noticed on the figure, especially the trails of start of linear behaviour of the stiff rock samples are easily noticeable.

3) Testing Method

During the testing utilised a heavily stiff testing machine connected to a computer data logger is used. No confining stress was applied during the UCS tests except the confining stress was applied using a Hoek cell during Balmoral-red granite samples. The axial load was applied using testing rig operating in displacement control at rate of 0.00625 mm/s by two

LVDTs (linear variable displacement transformers) with a precision of 0.005mm which were mounted in horizontal steel plates, securely attached to top and bottom of the testing platens (Dweirj, 2006). The two sets of LVDT readings were averaged to calculate the main axial displacement. The computer displayed real time plots of L-D throughout the test continuously monitoring and recording the axial load, axial displacement, confining stress and volumetric strain.

4) Test Specimen

Cylindrical samples cored and prepared from the same block of rocks in vertical orientation complying with the ISRM suggested standards. Tests of UCS leading to failure were conducted for the majority of the samples. The number and type of the tests conducted on the samples are presented in Table 1 with some of their physical specifications. The corresponding cross-sectional area (A) and length (L) of the specimens are also given in the table. The diameter and the length of the specimens were approximately 36mm and 73mm, respectively.

5) Results

L-D data of norite, granite, sandstone, limestone, marble, siltstone dry rock samples were used during the development and verification of the proposed

Table 1 Deviations between the real-time max bearable and calculated onset of failure stress data over different type of rock samples.

ROCK TYPE	ID	σ₃ (MPa)	Baseline of Data (kN)	SAMPLE'S PHYSICAL PROPERTIES			DIMENSIONS		Deviation from Max Bearable Force kN %		NUM OF TESTS	TYPE OF TEST
				Appearance	Stiffness	Breakage	Ave. Length	Ave. Area (mm²)	mean	std		
NORITE	South Africa	0	≥40	hazy-grey	very high	highly brittle	77.12	1032.26	1.019	0.889	4	UCS
GRANITE	Balmoral Red	2	≥50	red	high	brittle	76.14	1037.05	0.744	0.284	4	TRIAX
	Balmoral Red	4	≥50	red	high	brittle	75.39	1039.11	1.105	0.397	4	TRIAX
	Balmoral Red	6	≥100	red	high	brittle	75.38	1035.39	6.371	9.102	4	TRIAX
	Balmoral Red	8	≥100	red	high	brittle	75.20	1034.75	0.975	0.225	4	TRIAX
	Balmoral Red	10	≥100	red	high	brittle	75.23	1036.84	0.263	0.116	4	TRIAX
	Darkgrey	0	≥50	dark-grey	high	brittle	74.08	1075.14	0.460	0.509	4	UCS
	Darkgrey (weak)	0	≥15	dark-grey	low	brittle	76.14	1076.91	4.411	5.563	4	UCS
	Lightgrey	0	≥50	light-grey	high	brittle	71.19	1074.75	4.472	6.062	4	UCS
	Mt Sorrel	0	≥70	greyish	low	highly brittle	74.01	1063.22	9.207	9.394	8	UCS
	Canada	0	≥50	greyish	high	brittle	74.31	1041.70	0.643	0.681	3	UCS
GRANITE & GNEISS	I.C.C.			greyish with slightly layered yellowish grey mica bands	high	ductile	72.84	1076.96			8	UCS
		0	≥20						0.394	0.295		
SANDSTONE	Red	0	≥25	brownish-red	low	brittle	74.12	1036.45	2.046	2.183	4	UCS
	Peakmoor	0	≥25	buff	low	brittle	74.12	950.94	6.429	7.373	4	UCS
LIMESTONE	India	0	≥50	light-grey	medium	brittle	72.50	1078.38	4.600	3.576	38	UCS
	Chinese	0	≥40	dark-grey	medium	brittle	73.97	1051.67	13.377	7.778	9	UCS
SILTSTONE	Arkwright	0	≥62	light-grey	low	ductile	73.90	1066.83	4.302	5.397	27	UCS
MARBLE	France	0	≥25	white	medium	ductile	73.97	975.55	3.419	4.828	17	UCS

Based on the test results obtained from Rock Mechanics Laboratory of School of Civil Engineering of the University of Nottingham
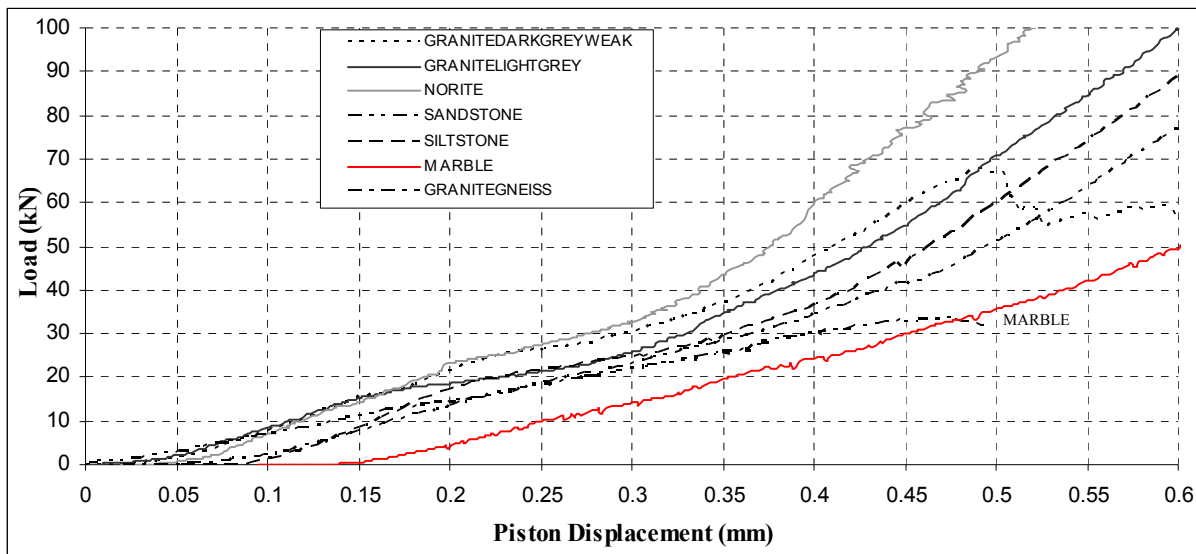
Fig. 6   Load-Piston displacement curves of some rock samples tested (after Reddish, 2008).

research approach. A pictorial representation of the L-D curve with its I/O parameters, during a UCS test is given in Figure 7.

The L-D curves breakdown points of the norite rock samples were mostly even, matching each other and varying between 350kN-0.35mm and 400kN-0.75mm. Since norite samples were very stiff and highly brittle, they can unexpectedly break during the test compared to the other rock types where it was really hard to locate the onset of failure points. The approach worked out rather well from three of the four UCS tests, at breaking points.

Tests carried out on five types of granite rock samples grouped according to their identifications are: Balmoral-red, dark-grey, light-grey, Mt. Sorrel and Canadian granite. The matching types of samples were cored from carefully selected locations of the same blocks. During real-time tests, the average values of load (kN) and displacement (mm) at failure points for each group vary between: (200-4.0) [σ_3 = 2MPa] and (340-0.6) [σ_3 = 10MPa], (210-0.3) and (220-0.32), (100-1.8) and (175-2.5), (140-0.78), (250-0.92) and (120-0.5), (170-0.7) respectively. The L-D curves of granite samples show larger variation so that the curves of dark-grey weak granite samples are in irregular trends of path and failure. The curves of Mt. Sorrel samples are extremely wavy with diverse trends of path and present unexpected failure points with low displacement data compared with Canadian samples which are in fairly close trends of path and points of failure. The applied approach presents comparatively higher variations at the failure points on UCS tested Mt Sorrel samples were presented higher deflections comparing to dark-grey (weak) and light-grey granite samples give close correlations with real-time data. Samples from Canada

were perfect accord with real-time data. Application of this approach on triaxially tested Balmoral-red samples were concordant with all steps of σ_3 treatment except for σ_3 = 6 MPa.

The L-D curves of the granite-gneiss rock samples showed regular elongated trend-lines with smooth trails and slight path deviations changing between 155kN-0.25mm and 195kN-0.75mm. The results were perfectly accord with the samples' points of disintegration.

Both types of sandstone rocks show a distinguishable feature of vague layers throughout the samples. The L-D changes of the red-sandstone samples demonstrated close trends through considerably even curves that varied between 32kN-0.35mm and 41kN-0.75mm. The L-D data of the Peakmooor sandstone samples exhibited close trends but undulating paths that showed variations between 35kN-0.18mm and 50kN-0.23mm, at collapse. The developed approach fitted well with the red-sandstone samples and presented acceptable limits of deviations on Peakmoor sandstone samples, at breakdown points.

Apart from a few test results, the L-D curves of the marble samples seem to follow parallel trend-lines with curly paths that show vast discrepancies of between 45kN-0.3mm and 84kN-0.6mm. The results of marble samples were quite close to failure points.

The Chinese limestone rock samples' L-D curves appeared to follow parallel trend-lines, except for a few, with highly twisted trails and had changing breakdown points between 155kN-0.4mm and 210kN-0.45mm. In general, the L-D curves followed parallel trend-lines with satisfactory trails and had highly changing breakdown points between 150kN-0.35mm and 250kN-0.45mm. The results of
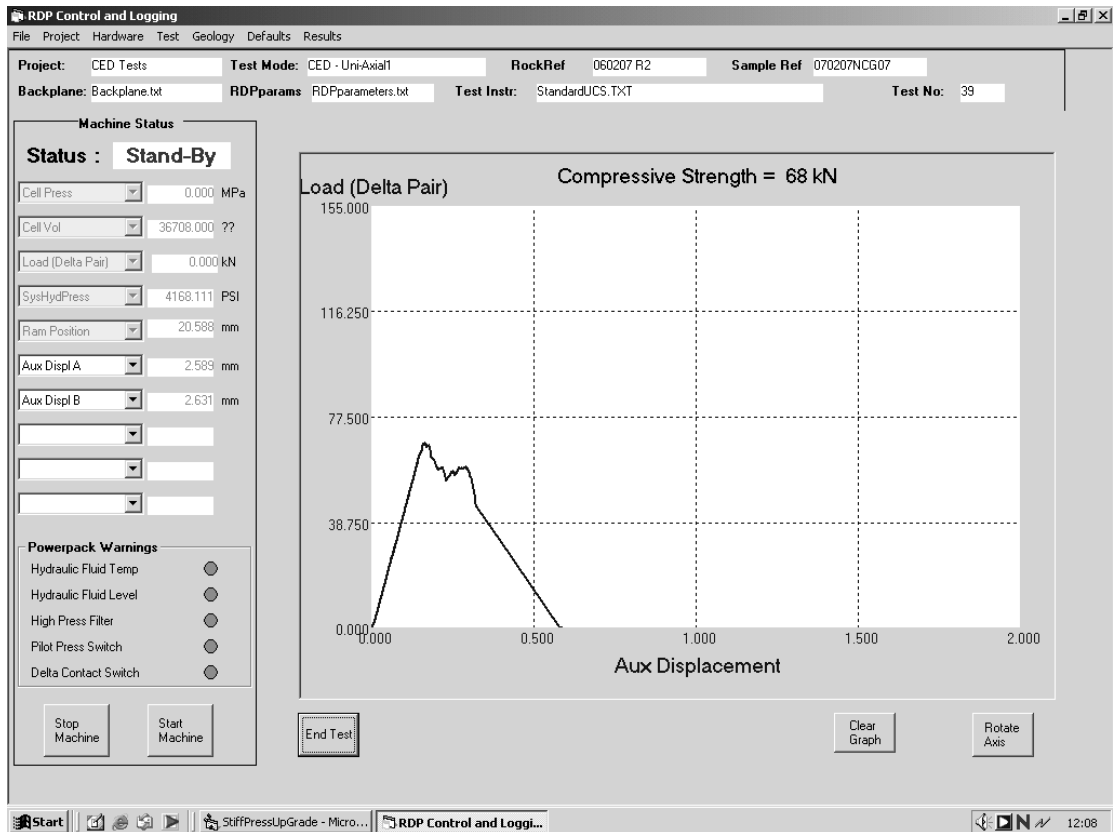
Fig. 7   Load-displacement curve of a dark-grey granite rock sample during UCS test (after Rowsell, 2005).

Chinese samples were a bit outside of the target (5 %) because of highly distorted nature of the L-D curves. In contrast, Indian limestone samples' results were in accord with failure points.

The siltstone samples were dominated by a similar angle of lamination. The L-D curves of the siltstone rock samples showed irregular trend-lines with wavy and diverse trails. The failure points changed between 140kN-0.8mm and 250kN-1.45mm. The siltstone samples' results were inside acceptable per cent of deviation from failure locations.

The main focus was to detect the onset of failure points by utilizing the slope of the characteristic L-D data with reasonable accuracy. L-D data curve paths showed great differences depending on rock type tested. Since the loading conditions were kept constant these discrepancies should refer to noises which can be attributed to the presence of pre-existing and induced cracks in the material during testing and to the mechanical and electrical machine noises recorded by the monitoring system. From the point of view of challenging examples in test data sets, although performance of the approach for different rocks was changing from sample to sample, there were almost none unpredictable samples using this method. The onset of failure points was not determined in a few tests because either the tests were not properly applied

or the samples were not appropriately prepared or the tests were not fully completed. The algorithm for the trigonometric screening of L-D data and prediction of nearby point were implemented using C program. A single run of the algorithm for a given rock took less than a second. The program is very efficient and it can be embedded into the main program interface was in MS Visual Basic.

CONCLUSIONS

In this study, a new approach is introduced to predict the onset of failure points of different types of rocks by evaluating L-D characteristics. In most cases, quantitative validation results show that less than 5 % mean deviation from maximum bearable stress measures of different type of rock samples. The average mean divergence from maximum bearable stresses achieved for 154 samples is around 3.5 %.

Historic L-D data was supplied by the University of Nottingham for norite, granite, sandstone, limestone, marble, siltstone rock samples and was examined during this research. First, the upper and lower trend lines of different group of samples for each type of rock were studied. The results illustrate the rock stiffness scale. The harder the rock types the steeper the upper and lower lines become. Initial attempts to represent L-D characteristics by a third degree polynomial equation using curve fitting of data

have failed. Observing that the onset of failure points is expected to be located where the linear behaviour of the rock ends, the study concentrated on the analysis of the L-D characteristics in the neighbourhood of elastic-plastic boundary of the graph.

The historic data supplied was studied during the development and verification of the technique which produces acceptable results on the same type of block samples for a given rock after assessing a single representative test.

Accurate determination of failure points is important because the sample is required to be intact during multiple failure state triaxial testing procedures to test the effect of minor principal stresses (σ_3) on rock stability. These test results may be important in understanding the load bearing capacity of intact rock which is crucial in the design stage of related engineering structures. There is strong evidence that using the developed approach features to identify curve characteristics is an accurate methodology to predict onset of failure points.

As yet, no comparison has been made to the currently employed method for determination of the onset of failure used by the University of Nottingham stiff testing machine.

REFERENCES

Bieniawski, Z. T.: 1967, Mechanism of brittle fracture of rock. Part I, Part II, Part, III. Int J of Rock Mech Min Sci, 4, 395–430.

Dweirj, K.M.: 2006, A study of stress dependent stiffness of rock using the multistage triaxial test. School of Chemical, Environmental and Mining Eng., PhD Thesis, the University of Nottingham, Nottingham.

Eberhardt, E., Stead, D. and Stimpson, B.: 1999, Quantifying progressive pre-peak brittle fracture damage in rock during uniaxial compression. Int J of Rock Mech Min Sci., 36, no. 3, 361–380.

Katz, O. and Reches, Z.: 2002, Pre-failure damage, time-dependent creep and strength variations of a brittle granite. Proc. 5th Int. Conf. on Analysis of Discontinuous Deformation, Ben-Gurion Univ., Balkema, Rotterdam.

Lajtai, E.Z.: 1972, Effect of tensile stress gradient on brittle fracture initiation. Int J of Rock Mech Min Sci & Geomech. Abs, 1972, 9, no. 5, 569–578.

Lama, R.D. and Vutukuri, V.S.: 1978, Handbook on Mechanical Properties of Rocks, 2, Testing Techniques and Results, Trans Tech Publications, Switzerland.

Lei, X.: 2006, Typical phases of pre-failure damage in granitic rocks under differential compression. Geological Society, Special Publications, London, 261, 11–29.

Martin, C.D. and Chandler, N.A.: 1994, The progressive fracture of Lac Du Bonnet granite. Int J of Rock Mech Min Sci. & GeoMech, Abs., 31, no. 6, 643–659.

Mogi, K.: 1966, Some precise measurements of fracture strength of rocks under uniform compressive stress. Rock Mech. and Rock Eng. Geology, 4, 41–55.

Ofoegbu, G.I. and Curran, J.H.: 1992, Deformability of intact rock. Int J of Rock Mech Min Sci. & Geomech. Abs., 29, no. 1, 35–48.

Perkins, R.D., Green, S.J. and Friedman, M.: 1970, Uniaxial stress behaviour of porphyritic tonalite at strain rates to 10^3/second. Int J of Rock Mech Min Sci. & Geomech. Abs., 7, no. 5, 527–535.

Ramamurthy, T.: 1986, Stability of rock mass. Indian Geotech. Jour., 16, no. 1, 1–75.

Reddish, D.J.: 2008, Test Data. Nottingham Centre for Geomechanics, Civil Engineering of the University of Nottingham, Nottingham.

Rowsell, P.J.: 2005, Documentation on the NCG Stiff Press Testing Machine, Nottingham Centre for Geomechanics, Department of Civil Engineering, University of Nottingham, Nottingham.

Tapponnier, P. and Brace, W.F.: 1976, Development of stress-induced microcracks in Westerly granite. Int J of Rock Mech Min Sci. & Geomech. Abs., 13, no. 4, 103–112.

Wawersik, W.R. and Fairhurst, C.: 1970, Study of brittle rock fracture in laboratory compression experiments. Int J of Rock Mech Min Sci., 7, no. 5, 561–575.

Yoshinaka, R., Yamabe, T. and Sekine, I.: 1983, Method to evaluate the deformation behaviour of discontinuous rock mass and its applicability. Proc. 5th Cong. of Int. Soc. for Rock Mechanics, Melbourne, 125–128.

Yumlu, M. and Ozbay, M.U.: 1995, Study of the behaviour of brittle rocks under plane strain and triaxial loading conditions. Int J of Rock Mech Min Sci., 32, no. 7, 725–733.